Lighting Direction Estimation in Perspective Shape from Shading by Genetic Algorithm

Chi Kin CHOW and Shiu Yin YUEN
City University of Hong Kong
Kowloon Tong, Hong Kong, China
{chowchi, kelviny.ee}@cityu.edu.hk

Abstract

In oblique shape from shading (SfS), the lighting (illumination) direction is essential for recovering the 3D surface of a shaded image. On the other hand, Fast Marching Methods (FMM) are SfS algorithms that use the mechanism of wave propagation to reconstruct the surface. In this paper, the estimation of lighting direction is addressed and we model it as an optimization problem. The idea is to minimize the inconsistency of wave propagation of FMM during the reconstruction. As the consistency of wave propagation is a multi-modal function, genetic algorithm (GA) is utilized to determine the lighting direction. Experimental results on four oblique SfSs with an unknown lighting direction are presented to demonstrate the performance of the proposed algorithm.

1. Introduction

Shape from shading (SfS) is an inverse process to determine the depth map D from its intensity image I based on the fact that there is a relation between D and I, i.e. $I = R(D)$. Due to the difficulty of the problem, typically five assumptions are made in the past: (1) Lambertian model; (2) orthographic projection; (3) a single light source placed at the infinity, which can be modeled as a lighting direction vector. The direction vector is assumed to be given a priori; (4) the boundary conditions or a good initial solution are a priori known. Sometimes, the more restrictive assumption: (5) frontal lighting, i.e. the lighting direction is perpendicular to the image plane, is also applied as Sfs reduces to a simpler Eikonal form in this case.

Recently, several articles reported solutions to relax the assumption of (2) to perspective projection, as the vast majority of images in reality are taken using perspective projection. Yuen et al. [4] proposed perspective SfS with the Fast Marching method (FMM) of [1]. This work is applied on images under frontal lighting. A one step, non-iterative approach is used that models the perspective effect directly. Another approach is reported by Courteille *et al.* [8], who also considered the case with frontal lighting and perspective projection. They used prior shape information to solve the equation. Tankus et al. [3] suggested the use of a perspective SfS based on the orthographic FMM of [1], in which the assumption of frontal lighting is relaxed. They used the FMM for orthographic projection as the initial solution, then used an iterative scheme for computing the perspective FMM. Wei and Hirzinger [9] applied multiplayer feedforward networks to solve the SfS problem. Since the algorithms employ gradient descent methods to optimize the error function, the solutions (depths) are not guaranteed to be globally optimal. In addition, over-smoothing will occur as [9] involves regularization in the surface recovery. Jezekiel et al. [10] proposed a shape from shading method based on learning spatially localized brightness pattern. Prados and Faugeras [11] introduced the perspective irradiance equation for solving the SfS problem, which can handle the cases of perspective projection and oblique lighting. They showed that both orthographic and perspective SFS (under frontal or oblique lighting) can be modeled by one generic Hamiltonian, and proposed an iterative scheme that is guaranteed to converge to the correct viscosity solution. Their algorithm is able to deal with discontinuities as well as shadows. However, the algorithm is iterative and the depth at the boundary and all the singular points must be given.

Considering the more general case of oblique lighting introduces the problem of lighting direction estimation. A useful discussion of the ambiguities involved in light source estimation can be found in [5].

Fourth Canadian Conference on Computer and Robot Vision(CRV'07)
0-7695-2786-8/07 $20.00 © 2007 IEEE

Several groups of researchers have proposed methods for the estimation of the lighting direction. Zheng and Chellappa [7] consider shadowing effects and use a uniform distribution of the tilt and slant angles of surface normals. They assume local spherical patches and their algorithm suffers on surfaces that deviate significantly from this assumption. Leclerc and Bobick [6] derive accurate light source information from surfaces reconstructed using stereo data. However, shape from stereo requires at least two images, which may simply not be available, for example, in a single photo. Recently, Ikeda [17] uses a Newton's iterative method with Jacobi update to solve the SfS problem. He estimates the lighting direction by maximizing a form of the rank condition in the update matrix. This implicitly assumes that the lighting direction that will best stabilize the iterative scheme is the correct direction. The assumption lacks a rigorous theoretical justification and may not be true in reality.

Cho and Chow [14] reports a neural computation approach to recover the reflectance model and the 3D shape of a shaded image. The model is an iterative approach: the estimated reflectance model and 3D shape are mutually updated by each another until the proposed stopping criterion is reached. Dimitris et. al. [16] propose an iterative algorithm and a deformable model to estimate the surface and lighting direction of a shaded image jointly. Similar to work of [14], The initialized lighting direction by [7] is passed to estimate the model parameters (surface). Afterwards, the lighting direction is re-estimated by feedback of the surface obtained in the pervious step. The iteration is repeated until the estimated lighting direction and the model parameters mutually agree. The accuracies of [14] and [16] highly depend on that the initial conditions and the deformable model parameter settings. Furthermore, there is no convergence proof of the algorithm, so we do not know whether the algorithms converge, let alone converge to the correct solution. In addition, how to determine the parameters of the deformable model in [14] in the first place is an unsolved problem.

In shape from shading, fast marching methods (FMMs) [1] [3] [4] are deterministic, non-iterative and the algorithm has complexity $O(NlogN)$ for a guaranteed correct surface reconstruction. The basic idea of the method is to systematically construct the solution using only upwind values. FMM can reconstruct the surface accurately provided that the depths of singular points are known. Our original perspective Sfs method [4] only works for frontal lighting. In this article, we extend the method to unknown non-frontal lighting. We also report a method to estimate the lighting direction using Genetic Algorithm (GA). We make the following assumptions: (1) Lambertian model, (2) perspective projection, (3) single light source at infinity, with unknown lighting direction, and (4) depths of single points are provided.

It relaxes the standard assumptions of Sfs in the following ways: (2) perspective projection is a more realistic assumption for practical imagery. (3) the lighting direction may now be oblique (non-frontal), and the lighting direction is assumed to be unknown. It may also be pointed out that for FMM based methods, the depths of image boundary do not need to be given in (4).

In this article, the lighting direction estimation is modeled as a two dimensional optimization. Since the proposed energy function is non-differentiable and consists of many local optimums, we optimize the energy function by a global optimization method: the Genetic algorithm. Empirical justification of the nature of the problem is given in the experimental results in section 5.

The rest of this paper is organized as follows: Section 2 briefly introduces the perspective FMM and a novel extension to handle oblique lighting under perspective projection. Section 3 presents a novel measure (fitness function) to describe the consistency of a lighting direction guess based on the nature of FMM. A novel GA-based approach to optimize the measure is discussed in section 4. Section 5 investigates the performance of the proposed algorithm on 4 sets of SfS problems and the nature of the fitness landscape of the problem, which provides justification for using GA. A comparison is also made with a simple gradient descent approach. A conclusion is drawn in section 6.

2. Fast Marching Method

Sethian [1] introduces the Fast Marching Method. It applies to phenomena that can be described as a wavefront propagating (normal to itself) with a speed $F = F(i, j)$. The main idea is to systematically construct the solution using only upwind values. Let the solution surface $T(i, j)$ be the time at which the curve crosses the point (i, j), then it satisfies the *Eikonal equation* $|\nabla T| = 1$. The physical meaning is that the gradient of arrival time of the front is inversely proportional to the speed of the front. For an upwind scheme, the approximation to the gradient is written as:

$$\left[\max(D_{ij}^{-x}T, -D_{ij}^{+x}T, 0)^2 + \max(D_{ij}^{-y}T, -D_{ij}^{+y}T, 0)^2\right]^{\frac{1}{2}} = \frac{1}{F_{ij}}$$

0-7695-2786-8/07 $20.00 © 2007 IEEE

where the difference operator notation, for example $D_{ij}^{+x}T = (T_{i+1,j} - T_{i,j})/\Delta x$ is employed. A key insight in this scheme is that to solve this nonlinear system, an optimal ordering of the grid points can be found. Starting at the singular points (also called boundary points), which are sources of the wave, the method marches the front outwards one grid point at a time. In detail, the method is as follows:

1. Assign the T values of all local minimum singular points. Label the singular points as *Known*.
2. Label as *Trial* all points that are one grid point away. Calculate the T value of the *Trial* points.
3. Label as *Far* all other grid points.
4. Determine the trial point A that has the smallest T value.
5. Remove A from *Trial* and add it to *Known*.
6. Label as *Trial* all neighbors of A that are not already *Known*, i.e., if the neighbor is in *Far*, removes, and add to the set *Trial*.
7. If all points are labeled as *Known*, then exit, else goto step 4.

Note that the T values of those local minimum singular points that are sources need to be given (step 1), and the point with the smallest T is updated (step 4). The later is known as the *entropy condition*. This condition is a consequence of the Fermat's principle of least time, taking the physical analogy that the propagating particles are light particles [13]. Computationally, the fast marching is the same as the well known A^* algorithm.

The FMM can be applied to perspective Sfs under frontal lighting. For details, the reader is referred to [4].

Lighting direction estimation involves the oblique lighting SfS which cannot be handled by existing FMMs. In order to overcome this limitation, we present a novel lighting transformation applied to the shaded image before performing FMM below: This transformation is based on the idea of coordinate transformation of [1]. It aims at estimating the image that is viewed at the direction of light source $[l_1, l_2, l_3]$ by means of which perspective SfS under oblique lighting can be simplified as those under frontal lighting.

Different from the orthographic projection case in [1], the coordinate transformation does not involve any approximation of z. So a more accurate result can be obtained. The details of the image transformation are discussed in the following:

Given that $I(u, v)$ and $D(u, v)$ are intensity and depth of the pixel (u, v) respectively, the corresponding 3D coordinate P in viewpoint coordinate system is

$$\left(\frac{uD(u,v)}{f}, \quad \frac{vD(u,v)}{f}, \quad D(u,v) \right)$$

On the other hand, the same point at the light-source coordinate system with lighting direction $[l_1, 0, l_3]$ is simply

$$\left(D(u,v)\left(l_1 \frac{u}{f} + l_3 \right), \quad D(u,v)\frac{v}{f}, \quad D(u,v)\left(-l_3 \frac{u}{f} + l_1 \right) \right)$$

where it is projected onto (u', v') of the transformed image plane I' under the perspective projection

$$(u', \quad v') = \left(\frac{f(l_1 u + l_3 f)}{-l_3 u + l_1 f}, \quad \frac{fv}{-l_3 u + l_1 f} \right)$$

Since the intensity is invariant to the coordinate system under the Lambertian model (i.e. depends only on the surface normal and lighting direction), the pixel $(u, v, I(u, v))$ is transformed as $(u', v', I(u, v))$ which is independent of D. In general, any $I(u, v)$ illuminated from $[l_1, l_2, l_3]$ can be transformed as $I'(u, v)$ illuminated from $[l_1, 0, l_3]$ by simply rotating $\tan^{-1}(l_2 / l_1)$. An oblique illuminated image is able to be transformed as the one viewed at the direction of light source by the two transformations:

$$I'(u', v') = T_I(I(u, v), [\alpha, \beta])$$

$$= I\left(\frac{f(l_1(r_1 u' + r_2 v') + l_3 f)}{-l_3(r_1 u' + r_2 v') + l_1 f}, \quad \frac{f(r_1 v' - r_2 u')}{-l_3(r_1 u' + r_2 v') + l_1 f} \right)$$

where $l_1 = \cos\alpha$, $l_3 = \sin\alpha$, $r_1 = \cos\beta$ and $r_2 = \sin\beta$.

3. Correct lighting direction is of consistent wave propagation

FMMs employ the mechanism of wave propagation to reconstruct the surface. Each singular point generates a wavefront for which the starting time of the propagation is the singular point depth value. In oblique SfS, an incorrect lighting direction will produce an incorrectly transformed image. Thus an incorrect 3D reconstruction result is expected. This leads to two possible incorrect wave propagations:

1. The propagation starts too fast or too slow (due to incorrect singular point depths).
2. The speed of propagation is higher or lower than the actual values (due to incorrect lighting direction that gives an incorrect Sfs equation).

These incorrect propagation lead to an inconsistency among the wavefronts or delays of wavefronts

collisions, in which the depth of an image point estimated by wavefront W_1 is different from that of another wavefront W_2. Alternatively, a set of correct wave propagation is equivalent to zero delay collisions of wave propagation. In more detail, suppose that **P** is a peak singular point and **Q** is the first visited singular point (FvSP) of the wavefront W_P of **P**, the depth of **Q** estimated by W_P should equal to actual depth of **Q**.

Motivated by the observation of consistent wavefront propagation, we propose to measure the correctness of an lighting direction estimation by the inconsistency of wavefronts. The inconsistency is defined as the differences among the estimated depths by wavefront and the actual depths of FvSPs of peak singular points, and inconsistency of a correct lighting direction is expected to be zero.

4. Genetic Algorithm

Genetic Algorithm (GA) attracts much attention from researchers due to its ability to find the global optimum of a complex, non-differentiable, non-smooth objective function. For this kind of landscapes, conventional optimization techniques are problematic and do not have good performance. GA is classified as a technique in Evolutionary Computation (EC) that searches the global optimum based on ideas from natural selection, crossover type information interchange during sexual reproduction, as well as random changes due to mutation. In the use of GA, (1) a suitable chromosome representation and (2) a suitable fitness function need to be designed before performing optimization. The designs are presented in the following:

4.1 Chromosome representation

Since the lighting direction **L** of a single light source at infinity can be represented by two angles, we define this set of angles as a chromosome. Each angle then corresponds to one of the genes in a chromosome. They are defined as: $\alpha \in [0°, 90°]$ = the angle between **L** and x-y plane and $\beta \in [0°, 180°]$ = the angle between **L** and x-z plane. Thus, a chromosome $\mathbf{C} = [\alpha, \beta]$ represents the lighting direction $[\cos\alpha\sin\beta, \cos\alpha\cos\beta, \sin\alpha]$.

4.2 Fitness function

A GA uses a fitness function to determine the performance of each artificially created chromosome. Since the fitness function is intended to measure the lighting direction quality, it is natural to use the inconsistency of wavefronts discussed in the previous section as the fitness function. Since the fitness function involves a SfS under oblique lighting, the shaded image has to be transformed by the lighting transformation (section 2) before each fitness evaluation. Suppose the target image $I(u, v)$ consists of n singular points $\{\mathbf{P_i} = [u_i, v_i, D_i]\}_{i \in [1, n]}$ (with known depths), the fitness F of a chromosome $\mathbf{C} = [\alpha, \beta]$ is defined as:

Fitness Function

Input: chromosome **C**

1. Transform $\{\mathbf{P_i}\}$ to $\mathbf{S} = \{\mathbf{Q_i} = [u_i', v_i', D_i']\}_{i \in [1, n]}$
2. Transform $I(u, v)$ to $I'(u', v') = T_I(I(u, v), \mathbf{C})$ using the lighting transformation T_I.
3. for $i := 1$ to n
4. Assume that $I'(u', v')$ consists of only one singular point $\mathbf{Q_i}$
5. Perform FMM on $I'(u', v')$ and denote the estimated depth map as $D_i(u', v')$.
6. Define $\mathbf{Q_{N(i)}} \in \mathbf{S}$ as the FvSP of $\mathbf{Q_i}$ where

$$\mathbf{N(i)} = \arg\min_{\substack{j \in [1,n] \\ j \neq i}} \left| D_i(u_i', v_i') - D_i(u_j', v_j') \right|$$

7. next i
8. $F(\mathbf{C}) = \sum f_i$ where f_i is the inconsistency of $\mathbf{Q_i}$:

$$f_i = \begin{cases} |D_{N(i)}' - D_i(u_{N(i)}', v_{N(i)}')| & \text{if } D_i' < D_{N(i)}' \\ 0 & \text{otherwise} \end{cases}$$

Output: fitness value $F(\mathbf{C})$ of **C**

Given a chromosome **C** that represents the possible lighting direction $[\alpha, \beta]$, the singular point set $\{\mathbf{P_i}\}$ is transformed as $\mathbf{S} = \{\mathbf{Q_i} = [u_i', v_i', D_i']\}_{i \in [1, n]}$. In addition, the shaded image $I(u, v)$ is transformed to $I'(u', v')$ using the proposed lighting transformation T_I. For each transformed singular point $\mathbf{Q_i}$, we perform a FMM on the $I'(u', v')$ and name the estimated depth map as $D_i(u', v')$. During the FMM, only the wavefront of $\mathbf{Q_i}$ is propagated. Meanwhile, the FvSP of $\mathbf{Q_i}$, namely $\mathbf{Q_{N(i)}} \in \mathbf{S}$, is defined based on the wavefront propagation. The inconsistency f_i of $\mathbf{Q_i}$ is denoted by the absolute difference between the desired and the estimated depth of $\mathbf{Q_{N(i)}}$, i.e. the absolute difference of $D_{N(i)}'$ and $D_i(u_{N(i)}', v_{N(i)}')$ if $\mathbf{Q_i}$ is the valley of $\mathbf{Q_{n(i)}}$, i.e. $D_i' < D_{N(i)}'$. Otherwise, f_i is assigned as zero in order to ignore its consistency. $F(\mathbf{C})$ is computed as the sum of the inconsistencies of all singular points.

0-7695-2786-8/07 $20.00

5. Experimental Results

In this section, the proposed algorithm is examined by a set of synthetic images that are obtained from 4 models: 4 Mountains, 3 Hill, Step and CosCos:

4 Mountains: See [4] for details

3 Hills:

$$z(\mathbf{x}) = 40e^{-\frac{\|\mathbf{x}-\boldsymbol{\mu}_1\|}{800}} + 40e^{-\frac{\|\mathbf{x}-\boldsymbol{\mu}_2\|}{800}} + 40e^{-\frac{\|\mathbf{x}-\boldsymbol{\mu}_3\|}{800}}$$

where

$\boldsymbol{\mu}_1 = [32,96]$, $\boldsymbol{\mu}_2 = [96,96]$ and $\boldsymbol{\mu}_3 = [64,32]$

Step:

$$z(\mathbf{x}) = 60S_1(x_1)S_2(x_2)$$

where

$$S_1(y) = \left(1+e^{-0.08(y-10)}\right)^{-1} + \left(1+e^{-0.2(y-96)}\right)^{-1}$$
$$S_2(y) = P_1y^2 + P_2y + P_3$$
$$P_1 = -1\times10^{-4},\ P_2 = 1.6\times10^{-2},\ P_3 = -1.59\times10^{-2}$$

CosCos:

$$z(\mathbf{x}) = 10z_1(\mathbf{x})(2 + z_2(\mathbf{x}))$$

Where

$$z_1(\mathbf{x}) = 1 - 0.5e^{-\frac{\|\mathbf{x}-\boldsymbol{\mu}\|}{8192}}$$
$$z_2(\mathbf{x}) = \cos\left(\frac{4\pi x_1}{128}\right)\cos\left(\frac{4\pi x_2}{128}\right)$$
$\boldsymbol{\mu} = [64,64]$

The second column of Figure 2 shows the 4 examined models. The focal lengths and offsets for rendering the shaded images are listed in Table 1.

Table 1. The focal lengths and offsets for rendering the synthetic images

	Focal length	Offset
4 Mountains	70	200
3 Hills	60	200
Step	70	200
CosCos	60	200

The shaded images (the first column of Figure 2) are generated by the method of [4]. The sizes of the shaded images are 128 by 128 and the desired oblique angles are $\alpha = 20°$ and $\beta = 40°$, i.e. $\mathbf{L_a} = [20, 40]$. In this experiment, the perspective FMM of [4] is employed in the fitness evaluation and shape recovery.

The population size of GA is chosen as 40. The evolution is terminated after 60 generations. The genetic operators and the selection scheme of GA follow those in [15]. Since the search space of this application is relatively smaller than that of [15], the search space contraction of [15] is not applied in this experiment. The accuracy of the estimated lighting direction $\mathbf{L_e}$ is evaluated by the following quantities:

1. L_2: L_2 norm distance between $\mathbf{L_a}$ and $\mathbf{L_e}$
2. θ: Angle between $\mathbf{L_a}$ and $\mathbf{L_e}$, $\theta = \cos^{-1}(\mathbf{L_a} \cdot \mathbf{L_e})$.
3. D_{mean}: The average absolute differences between the actual depth map $D_a(u, v)$ and the estimated depth map $D_e(u, v)$ obtained by $\mathbf{L_e}$. Due to the discontinuities around the silhouettes (depth discontinuities) of the tested models, it is expected that huge errors occur at those regions. In order to illustrate the performance of the algorithms in a conclusive manner (i.e. ignore the meaningless solution at the silhouette), D_{mean} considers only the valid pixels. *(u,v)* is valid for computing D_{mean} if none of the pixel within the template centred at P is a silhouette pixel. Figure 1 shows an example of pixel validation with template width w = 3. Given that white-filled boxes represent the pixels with depth values, the solid-line boxes are regarded as the valid pixels for measuring the D_{mean} while the dotted-line boxes are the invalid pixels that are ignored in the calculation of D_{mean}. In this article, the template width w is assigned as 5.
4. D_{median}: The median of absolute difference of the valid pixels between $D_a(u, v)$ and $D_e(u, v)$.

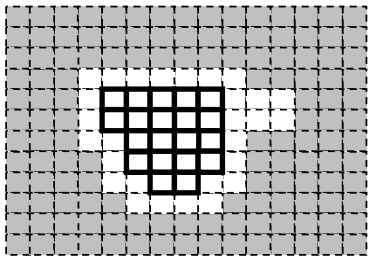

Figure 1. Example of pixel validation

The performance of the proposed algorithm is compared with the gradient descent method. Since the objective function (see sec. 4.2) is non-differentiable, a first order gradient approximation is employed:

$$\nabla F([\alpha,\beta]) = \left[\frac{F([\alpha+\Delta\alpha,\beta]) - F([\alpha-\Delta\alpha,\beta])}{\Delta\alpha},\ \frac{F([\alpha,\beta+\Delta\beta]) - F([\alpha,\beta-\Delta\beta])}{\Delta\beta}\right]$$

The solution $\mathbf{C}$ is updated as $\mathbf{C}^{(t+1)} = \mathbf{C}^{(t)} - \eta\nabla F(\mathbf{C}^{(t)})$ iteratively until the magnitude of the change of C is smaller than a predefined stopping threshold ε, i.e. $|\nabla F(\mathbf{C})| < \varepsilon$. The values of η and ε are chosen as 0.001 and 0.2 respectively by trial and error.

Since GA is a stochastic method, the four quantities: L_2, θ, D_{mean} and D_{median} are obtained by statistics gathered through 100 independent trials.

Similarly, 100 independent trials are applied to the gradient descent method, in which the initial starting points are randomly generated. The third and the forth columns of Figure 2 show typical estimated depth maps and the corresponding error maps. Seen from the figures, the proposed algorithm successfully recovers the lighting directions and hence accurately estimates the depth maps. Tables 2 - 5 list the accuracies of the proposed algorithm and the gradient descent method (indicated as M_1 and M_2 respectively) on the four 3D reconstructions. Seen from the tables, the proposed algorithm is vastly superior to the gradient descent method in all of the four accuracy measures. This is attributed to the nature of the proposed objective function: i.e. it is a multi-modal function with a single global optimum and many local optima (see below for empirical evidence for the above claim). In addition, the performance of the gradient descent method highly depends on the choice of initial starting point, step size and learning rate, and these results in erroneous estimations of lighting directions and depth maps. The much smaller standard deviations of the four measurements empirically indicate the higher reliability of the proposed algorithm compared with the gradient descent method.

Table 2. L_2 measurement of M_1: the proposed algorithm and M_2: gradient descent method. (a) 4 Mountains, (b) 3 Hills, (c) Step and (d) CosCos.

	Mean		Std.		Median	
	M_1	M_2	M_1	M_2	M_1	M_2
(a)	0.2°	18.3	0.02	2.34	0.17	17.1
(b)	1.6	23.3	0.03	1.87	1.4	22.6
(c)	0.8	25.8	0.02	3.05	0.6	24.3
(d)	1.3	21.8	0.13	4.71	1.1	20.1

Table 3. θ measurement of M_1: the proposed algorithm and M_2: gradient descent method. (a) 4 Mountains, (b) 3 Hills, (c) Step and (d) CosCos.

	Mean		Std.		Median	
	M_1	M_2	M_1	M_2	M_1	M_2
(a)	0.29°	25.71°	0.03°	2.71°	0.26°	24.6°
(b)	2.37°	33.81°	0.04°	20.8°	2.27°	33.1°
(c)	1.14°	33.62°	0.02°	3.13°	1.06°	31.2°
(d)	1.71°	31.4°	0.19°	4.67°	1.61°	30.8°

Table 4. D_{mean} measurement of M_1: the proposed algorithm and M_2: gradient descent method. (a) 4 Mountains, (b) 3 Hills, (c) Step and (d) CosCos

	Mean		Std.		Median	
	M_1	M_2	M_1	M_2	M_1	M_2
(a)	1.87	19.8	0.17	2.1	1.68	20.3
(b)	3.57	25.1	0.31	1.8	3.31	24.8
(c)	2.31	27.8	0.26	1.7	1.97	26.1
(d)	3.42	23.4	0.30	2.2	3.14	22.9

Table 5. D_{median} measurement of M_1: the proposed algorithm and M_2: gradient descent method. (a) 4 Mountains, (b) 3 Hills, (c) Step and (d) CosCos.

	Mean		Std.		Median	
	M_1	M_2	M_1	M_2	M_1	M_2
(a)	1.02	16.8	0.16	1.8	0.98	15.9
(b)	1.73	21.7	0.19	1.3	1.65	20.1
(c)	1.61	23.5	0.17	1.6	1.51	22.5
(d)	1.65	21.1	0.16	1.9	1.34	21.4

Figure 3 show the typical fitness landscapes of the 4 models. x and y-axis of the figures indicate the values of α and β respectively. Higher intensities denote lower fitness values of a possible solution and vice versa. (In this case, the fitness value is the value of the consistency measure, i.e. the lower the fitness values the better). In order to illustrate the distribution of the optima more clearly, the fitness values are in log scale. The brightest point indicates the global optimum. It is observed that the fitness landscapes are non-smooth and consist of multiple local optima and a single global optimum. These observations empirically illustrate the problem complexity and hence the suitability of an evolutionary computation approach such as the GA on solving this problem.

6. Conclusions

Shape from shading (SfS) refers to 3D shape recovery based on the shading information of an image. In SfS, fast marching methods (FMMs) [1] [3] [4] are deterministic, non-iterative and the algorithm has complexity $O(NlogN)$ for a guaranteed correct surface reconstruction. In this article, the proposed algorithm relaxes two assumptions of FMM: (1) orthographio projection is relaxed to the more realistic perspective projection; (2) known lighting direction is relaxed to unknown lighting direction that may be oblique or frontal. This enables the extended FMM to reconstruct surfaces under more realistic conditions. The assumption of frontal lighting is relaxed by applying a simple image transformation. We also point out that the consistency of wavefront propagation of FMM is a promising correctness measure for a lighting direction. Incorporating the GA, the lighting direction of a shaded image can be estimated by optimizing a two-dimensional objective function.

The experimental results support the contributions of this article. The plot of the fitness landscape

empirically illustrates the problem complexity and hence the suitability of an evolutionary computation approach such as the GA for solving this problem. Relaxation of the assumption of known singular point depths will be considered in future development.

Acknowledgment

The work described in this article was supported by a grant from CityU (7001707).

References

[1] R. Kimmel and J. A. Sethian, Optimal algorithm for shape from shading and path planning, *Journal of Mathematical Imaging and Vision*, vol. 14, no. 3, pp. 237 – 244, 2001.

[2] P. Dupuis and J. Oliensis, An optimal control formulation and related numerical methods for a problem in shape reconstruction, *The Annals of Applied Probability*, vol. 4, no. 2, pp. 287 – 346, 1994.

[3] A. Tankus, N. Sochen and Y. Yeshurun, Shape- from-shading Under Perspective Projection, *International Journal of Computer Vision*, vol. 63, no. 1, pp. 21 – 43, 2005.

[4] S.Y. Yuen, Y.Y. Tsui and C.K. Chow, A Fast Marching Formulation of Perspective Shape from Shading under Frontal Illumination, to appear in *Pattern Recognition Letters*, 2007. A preliminary version appears in S. Y. Yuen, Y. Y. Tsui, Y. W. Leung and M. M. Chen, Fast marching method for shape from shading under perspective projection, *Proc. of the 2nd IASTED Int'l Conf. Visualization, Imaging and Image Processing*, pp. 584 - 588, 2002.

[5] P. N. Belhumeur and D.J. Kriegman, What is the Set of Images of an Object under all Possible Lighting Conditions, *IEEE Computer Vision and Pattern Recognition*, pp. 270-277, 1996.

[6] Y. G. Leclerc and A. F. Bobick, The Direct Computation of Height from Shading, *IEEE Computer Vision and Pattern Recognition*, pp. 552-558, 1991.

[7] Q. Zheng and R. Chellappa, Estimation of Illuminant Direction, Albedo, and Shape from Shading, *IEEE Trans. Pattern Analysis and Machine Intelligence*, vol. 13, no. 7, pp. 680-702, July 1991.

[8] F. Courteille, A. Crouzil, J-D Durou and P. Gurdjod, Towards shape from shading under realistic photographic conditions, *Proc. of the 17th International Conference of Pattern Recognition*, vol. 2, pp. 277 – 280, 2004.

[9] Guo-Qing, Wei and gerd Hirzinger. Paramtric Shape-from-Shading by Radial Basis Functions, *IEEE Transactions on Pattern Analysis and Machine Intelligence*, vol. 19, no. 4, 1997.

[10] Jezekiel Ben-Arie and Dibyendu Nandy, A Neural Network Approach fro Reconstructing Surface Shape from Shading, *Proc. of International Conference on Image Processing*, vol. 2, pp. 972 – 976, 1998.

[11] E. Prados and O. Faugeras, A Generic and Provably Convergent Shape-from-Shading Method for Orthograhphic and Pinhole Cameras, *IJCV*, Vol. 65(1/2), pp. 97-125, 2005.

[12] E. Prados and O. Faugeras, Shape from Shading: a Well-posed Problem? *Proc. CVPR*, Vol. 2, pp. 870-877, 2005.

[13] P. W. Verbeek, B. J. H. Verwer, Shape from shape, the eikonal equation solved by gray-weighted distance transform. *PRL*, vol. 11, 681-690, 1990.

[14] Siu-Yueng Cho and T. W. S. Chow, Neural computation approach for developing a 3D shape reconstruction model**,** *IEEE Transactions on Neural Networks*, vol. 12, Issue 5, pp. 1204 – 1214, 2001

[15] Chow C. K., Tsui H. T. and Lee T., Surface registration using a dynamic genetic algorithm, *Pattern Recognition*, vol. 37, no. 1, pp. 105 – 117, 2004

[16] D. Samaras and D. Metaxas, Incorporating Illumination Constraints in Deformable Models for Shape from Shading and Light Direction Estimation, *IEEE Transactions on Pattern Analysis and Machine Intelligence*, vol. 25, no. 2, pp. 247 – 264, 2003.

[17] O. Ikeda, Shape-from-Shading for Oblique Lighting with Accuracy Enhancement by Light Direction Optimization, *EURASIP Journal on Applied Signal Processing*, pp. 1-10, 2006.

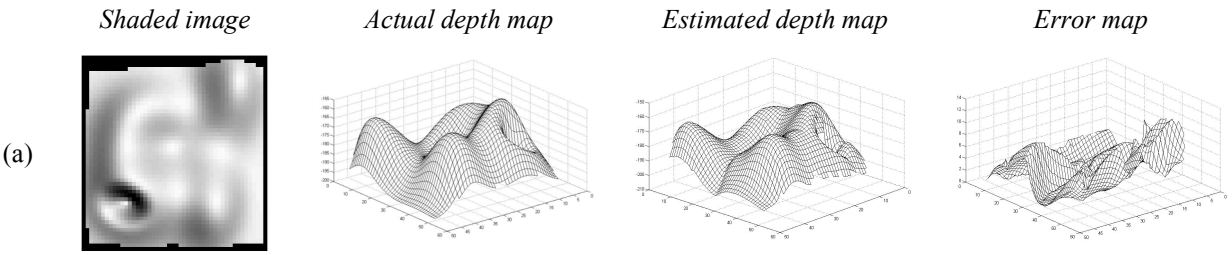

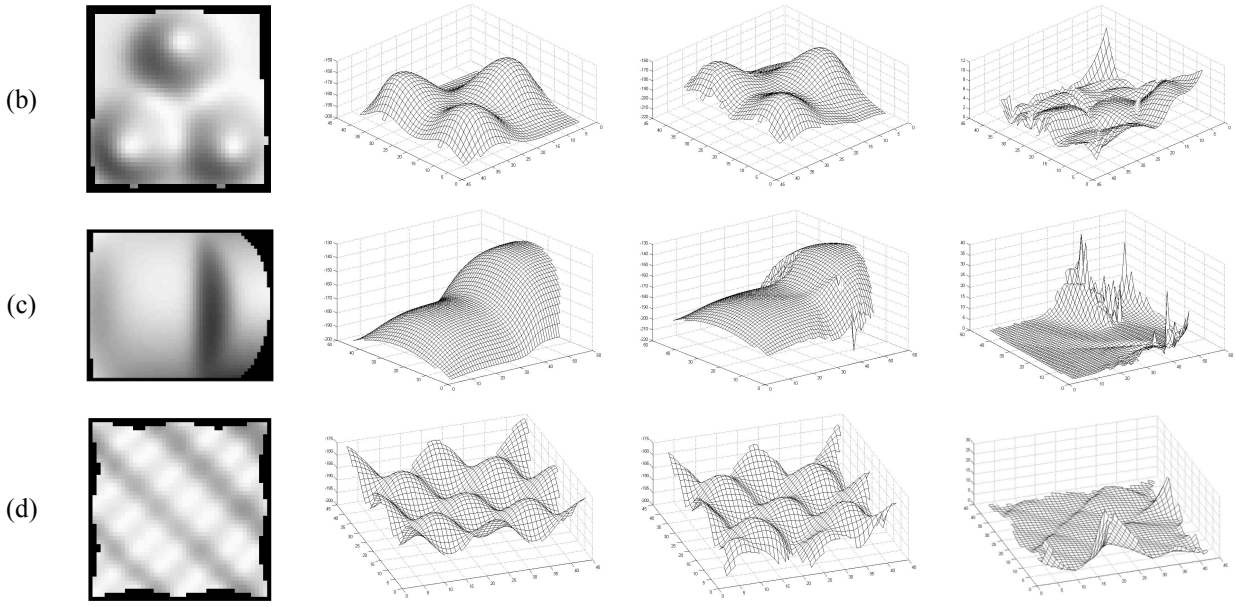

Figure 2. Experiment details: (a) 4 Mountains, (b) 3 Hills, (c) Step and (4) CosCos

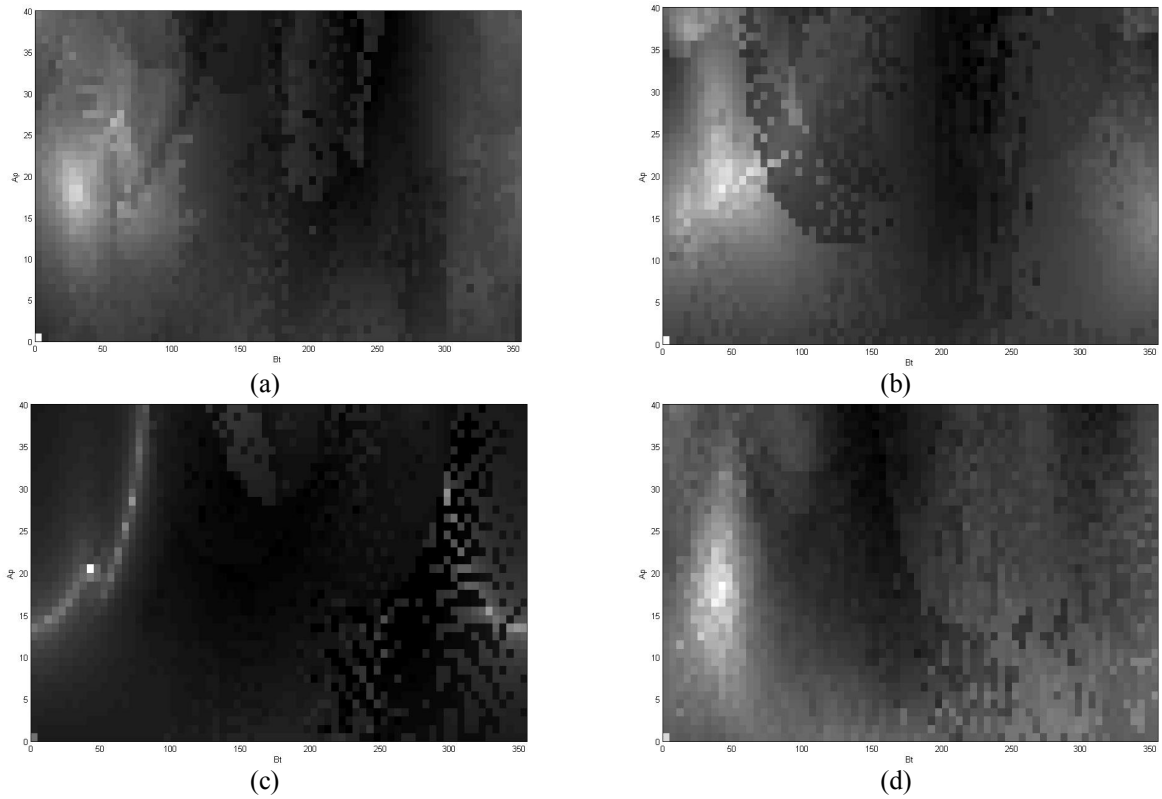

Figure 3. Fitness lanscapes of the experiment (a) 4 Mountains, (b) 3 Hills, (c) Step and (4) CosCos